Comparative Specular X-ray Reflectivity, Positron Annihilation Lifetime Spectroscopy, and Incoherent Neutron Scattering Measurements of the Dynamics in Thin Polycarbonate Films

Christopher L. Soles,* Jack F. Douglas, and Wen-li Wu

NIST Polymers Division, Gaithersburg, Maryland 20899-8541

Huagen Peng[†] and David W. Gidley[‡]

Department of Materials Science and Engineering and Department of Physics, University of Michigan, Ann Arbor, Michigan 48109-1120

Received October 19, 2003; Revised Manuscript Received January 15, 2004

ABSTRACT: There are many technological applications using thin polymer films that would be crucially influenced by confinement-induced changes in the transport properties of the film. In the present, we utilize specular X-ray reflectivity (SXR, to measure film thickness h), beam positron annihilation lifetime spectroscopy (PALS, to measure the nanometer-sized domains of unoccupied volume v), and incoherent neutron scattering (INS, to measure the mean-square atomic displacements $\langle u^2 \rangle$) to quantify the influence of film thickness in thin polycarbonate (PC) films. The thermal expansion coefficients of both h and v, as well as the amplitudes of $\langle u^2 \rangle$, indicate that thin film confinement affects reduced molecular mobility in PC. This reduced mobility is not necessarily reflected in the apparent glass transition temperature (T_g) derived from the same techniques. Specifically, SXR and PALS indicate a weak suppression of apparent T_g (the kink in the thermal expansion curve) when the film thickness becomes less than 200 Å, which should not be interpreted to imply enhanced mobility. The INS measurements confirm this by demonstrating that the kink in $\langle u^2 \rangle$ vs T (designated operationally as T_g) tends to disappear, possibly even increasing to higher T for film thinner than 500 Å. The reduced thermal motion can nominally be parametrized in terms of an immobilized region next to the rigid substrate, extending approximately 40−130 Å into the film, depending on the measurement technique and temperature range.

Introduction

Recently, there have been an increasing number of theoretical and experimental efforts to understand the physical properties of thin polymer films. Identifying the glass transition temperature (T_g) as a function of film thickness is a common theme, believed to impact numerous thin film applications since T_g traditionally implies a dramatic softening of the material. Keddie and Jones used ellipsometry to report the first decrease of T_g with thickness for polystyrene (PS) films supported on hydrogen-passivated Si substrates.[1,2] Soon after, the glass transition in supported PS films was studied by a range of experimental methods, including (but not limited to) ellipsometry,[3,4] Brillouin scattering,[4,5] positron annihilation,[6] specular X-ray reflectivity,[7−9] dielectric spectroscopy,[10,11] thermal probe analysis,[8,12] and atomic force microscopy.[13−15] While recent reviews[4,16] state that T_g always decreases with decreasing film thickness for these supported PS films, there are still a few reports that do not conform to this generalization.[7,8,14] Nevertheless, the prevailing view is that the T_g of thin supported polymer films is reduced on a weakly interacting substrate and increased when the thermodynamic interactions are strongly favorable, as now indicated in several thin film systems.[2,8,9,12,17] This view also seems to be supported by recent computer simulation studies.[18−20] Recent ellipsometry measurements on freely standing films indicate larger apparent T_g decreases[3,16,21,22] than substrate-supported films, presumably due to the presence of two free surfaces.

The phenomenology relating the glass transition through thermal expansion, specific volume, heat capacity, and related thermodynamics parameters is well established. It is, however, not clear to what extent these parameters reflect the molecular level dynamics in these polymer films; i.e., a molecular understanding of the glass transition is lacking. A "kink" in the temperature dependence of such a thermodynamic variable provides an operational definition of T_g, but in practice the dramatic decrease in modulus and increase in molecular mobility are the most relevant changes implied by the transition. Given that there is no generally accepted theory of glass formation, even in bulk materials, it is prudent to carefully examine what properties or parameters are appropriate for estimating changes in the level of molecular dynamics in thin polymer films. It is, moreover, not even clear whether the glass transition has a unique definition in highly confined thin films, and a completely new framework for describing glass formation may even be required.

Confinement also affects the thermal expansion coefficient, which is directly related to the modulus and mobility of thin polymer films. However, the manner in which thermal expansion changes with film thickness is difficult to reconcile (even qualitatively). In supported films, specular reflectivity shows that the coefficient of thermal expansion (β) decreases in either the melt,[7,23] the glass,[24] or both.[25] This contradicts ellipsometry studies on supported films where β increases with film thickness in the glassy state[1,2,4] and is independent of film thickness in the rubbery state. The increased β for glassy films is rationalized in terms of a "liquidlike" layer (of reduced T_g) at the free surface. However,

[†] Department of Materials Science and Engineering.
[‡] Department of Physics.

10.1021/ma035579a CCC: $27.50
Published on Web 03/24/2004

ellipsometry measurements on free-standing polystyrene (PS) films (with two free surfaces) show that β is independent of film thickness in the glass but decreases significantly with confinement in the melt.[16] Clearly there is considerable debate as to how confinement affects the thermal expansion behavior of thin films. On the basis of these observations, it is our view that a coherent interpretation or understanding of the finite size effects on glass formation is still lacking.

In this study, we employ three independent tools to probe the thermophysical affects of confinement in thin polycarbonate (PC). Two of these techniques, specular X-ray reflectivity (SXR)[7,23−25] and positron annihilation lifetime spectroscopy (PALS),[6] are well documented for studying the glass transition in thin polymer films while the third, incoherent neutron scattering (INS), is relatively new.[30−33] For consistency, all of the PC films are made in one lab and studied under identical conditions. The primary focus of this paper is to compare the different measurement techniques and discuss the implications of the various similarities and differences of their observations.

Experimental Section

Specular X-ray Reflectivity. Specular X-ray reflectivity (SXR) is used to track the expansion and contraction of the PC films (film thickness) as a function of temperature. The reflectivity curves are obtained using a modified Scintag[34] diffractometer (Scintag, Santa Clara, CA) with Ni-filtered Cu Kα radiation and a temperature-controlled sample stage stable to ±0.2 °C (absolute range of fluctuation around the set point). X-ray reflectivity curves under a vacuum of 10^{-4}−10^{-5} Pa are obtained on heating and cooling cycles between 20 and 200 °C in 20 °C steps. After each temperature change 45 min is allowed for thermal equilibration, followed by 1 h to acquire each isothermal reflectivity curve. The film thickness is obtained from the periodicity of the reflectivity fringes using a least-squares recursive fitting routine.[35]

Positron Annihilation Lifetime Spectroscopy. PALS characterizes the domains of low electron density in a polymeric material.[36,37] The orthopositronium (o-Ps) triplet will preferentially localize in the larger electron deficient regions (i.e., interchain "voids") characteristic of amorphous polymers. The o-Ps annihilation lifetime (τ_{Ps}) is approximately 1−3 ns in polymers, increases with the size of the packing defects, and corresponds to packing inefficiencies 5−10 Å in diameter. These nanovoid regions typically expand with temperature, exhibiting a linear increase in τ_{Ps} marked by a discontinuity in the derivative of the thermal expansion at the glass transition. The PALS technique has been adapted to study submicron polymer films by implementing a variable energy positron beam that controls the implantation depth of the positron.[6,38−40] In each thin film the positron beam energy E (keV) is adjusted to attain the maximum o-Ps formation rate. The resulting mean Ps implantation depth $\bar{Z}$ (Å) is given approximately by[41]

$$\bar{Z} = \frac{400}{\rho} E^{1.6} \tag{1}$$

where ρ (g/cm^3) is the film density. This optimized implantation energy typically corresponds to an implantation depth of roughly one-half the film thickness.

Silicon-supported PC films are introduced into the high vacuum ($\approx 5 \times 10^{-6}$ Pa) chamber of the University of Michigan beam-PALS apparatus and thermally cycled between 20 and 200 °C, normally in increments of 20 °C. At each increment, 3−6 h is required to collect a typical PALS spectrum. The average o-Ps lifetime, τ_{Ps}, is fitted from the spectrum with the PFPOSFIT fitting program.[42] The system time resolution is about 0.5 ns, more than sufficient to resolve the 2−3 ns o-Ps lifetime in PC. To reduce the statistical error and ensure reproducibility, several (2−3) thermal cycles are averaged to create a τ_{Ps} thermal expansion curve. The normalized slope of the lifetime vs temperature (this quantity is divided by τ_{Ps} at the fitted apparent T_g) defines the expansion coefficient, which is approximately the linear expansion volume coefficient for the cavities occupied by the o-Ps atom.[6]

Incoherent Neutron Scattering. At absolute zero, where atomic/molecular mobility is completely frozen, the incoherent neutron scattering (INS) from a polymer is purely elastic. As temperature increases, thermally activated dynamics lead to a decrease in intensity of the elastic scattering and a corresponding increase in the inelastic scattering. The temperature dependence of the elastic scattering is approximated with the Debye−Waller factor:

$$I_{inc}(Q) \propto e^{-(1/3)Q^2\langle u^2\rangle} \tag{2}$$

where Q is the scattering vector and $\langle u^2\rangle$ is the amplitude or mean-square atomic displacement of the thermally activated motions. In this framework, the slope of $\ln(I_{inc}(Q))$ vs Q^2, which can be tracked as a function of temperature, yields $\langle u^2\rangle$.

The INS experiments are done at the NIST Center for Neutron Research on the high-flux backscattering spectrometer (HFBS) located on the NG2 beamline.[43] This spectrometer has an energy resolution of 0.85 μeV, which means that $\langle u^2\rangle$ reflects motions that are 200 MHz or faster; slower motions appear as elastic scattering. The INS signal is dominated by H, which has a scattering cross section ≈20 times larger than that of either C or O and nearly 40 times larger than that of Si. In other words, the polymer film should dominate the incoherent scattering for our PC films supported on Si wafers. To obtain sufficient scattering signal from the thin films, several (13−15) Si wafers (75 mm in diameter) were broken into rectangular strips and placed in a sample cell (≈1−10 mg of PC in the cell). The spectrometer operates with a neutron wavelength of 6.271 Å over a Q range of 0.25−1.75 Å^{-1} (note: efforts were not made to control the orientation of the sample relative to Q). The fact that the first Bragg peak for Si occurs at $Q \approx 2.67$ Å^{-1} further ensures that the dynamics of the Si substrates contribute negligibly to the scattering intensity. The INS experiments are performed by thermally ramping the films at 0.1−0.5 °C/min from −223 to 250 °C. The elastic scattering intensities are recorded as a function of Q in temperature bins of 5−10 °C. As with the SXR and PALS experiments, the INS measurements are done in a vacuum (approximately 10^{-5} Pa).

Thin Film Preparation. The PC thin films for the SXR, PALS, and INS measurements are prepared under identical conditions in the NIST laboratory. PC, GE Plastics GE ML 4535-111N ($M_{w,r}$ = 36.3 kg/mol;[44] PDI ≈ 1.4]), is dissolved in cyclohexanone (Aldrich, 98.8% assay) at mass fractions ranging from 0.28% to 5.00% and filtered through a 0.45 mm Teflon filter. The dust-free solutions are then spun-coat at 2000 rpm for 40 s onto clean Si wafers (both ⟨111⟩ and ⟨100⟩ orientations were used). The Si wafers were prepared with a 5−15 Å thick hydrophilic oxide surface by removing organic residue in an O_2 plasma cleaner (Plasmaline, Tegal Corp.), stripping the native oxide with HF acid (J.T. Baker CMOS electronic grade; 48.8−49.2% assay), and then regrowing a uniform oxide surface through a 5 min UV-ozone exposure (UVO model 42, Jelight Co., Inc.). The PC films are then spun-coat immediately to minimize the chance of contaminating the clean surfaces. Prior to any measurements, the films are held for 6−12 h at 200 °C under a vacuum of 10^{-4}−10^{-5} Pa to remove residual casting solvent.

Results

Figure 1 summarizes the SXR thin film thickness measurements as a function of temperature T. The expansion curves are presented in terms of the percent change in film thickness relative to a reference thickness, $\delta h/h_0$ (arbitrarily the reference T is defined to be 180 °C). Each curve represents an average of 2−4

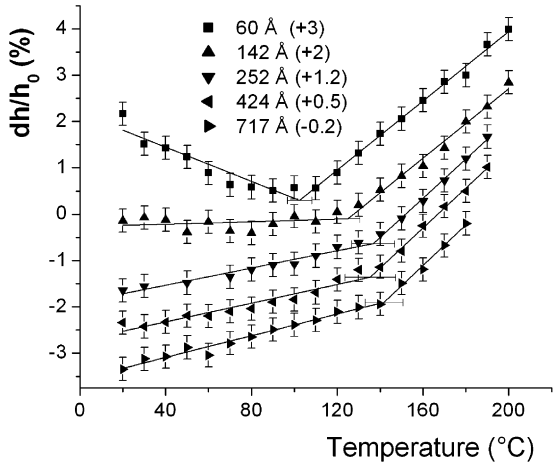

Figure 1. Change in film thickness δh as measured by specular X-ray reflectivity, in reference to the overall thickness at 180 °C (h_0). The curves are offset vertically for clarity by a value indicated in the legend. The extrapolated intersection of the fits, indicated by the solid lines, defines the apparent $T_{g,x}$, as described in the text. The error bars indicate standard uncertainties in film thickness, as described in the text.

heating and/or cooling cycles, with a slight vertical offset (by a constant indicated in the legend) added for clarity. The uncertainty of ±0.25% (indicated by the error bars) is defined as the average range of the 2−4 isothermal thickness measurements, averaged over all isothermal data sets. SXR cannot be used to measure expansion of a bulk reference. However, in the 717 Å film, a "kink" at 142 ± 9 °C in the expansion curve roughly coincides with the bulk calorimetric T_g of PC ($T_{g,c}$ = 150 °C). By convention, linear fits above and below this region, indicated by the solid lines, are used to establish the intercept or "kink" that is designated as the apparent glass transition $T_{g,x}$, as measured by X-ray reflectivity. To ensure an unbiased choice of $T_{g,x}$, we assume that the entire curve must be fit by two intersecting linear functions. A least-squares fitting algorithm is employed to vary both the slopes and intercept of the two linear functions. (The error bars on all apparent T_g's indicate one standard deviation of this fit.) As indicated by the remaining linear fits in Figure 1 and summarized in Table 1, $T_{g,x}$ measured by this method appears to decrease slightly (about one standard deviation) as the film thickness is diminished to 142 Å, and the effect is significant for the thinnest (60 Å) film.

The expansion coefficients for the glassy ($\beta_{x,g}$) and rubbery ($\beta_{x,r}$) regions (i.e., below and above $T_{g,x}$, respectively) are also reported in Table 1. The fitted values of $\beta_{x,r}$ are statistically consistent with little or no trend with film thickness. However, $\beta_{x,g}$ shows a marked decrease for thinner films and even becomes negative in the 60 Å film. While a comprehensive understanding or description of the negative $\beta_{x,g}$ is beyond the scope of this paper, we refer the interested reader to the accompanying paper in this issue where the negative $\beta_{x,g}$ is discussed in greater detail. Obviously, the fact that $\beta_{x,g}$ becomes negative is a concern for the apparent $T_{g,x}$ assessments in the thinnest films. We acknowledge this but note that $\beta_{x,r}$ is consistent with the thicker films in the region above the negative $\beta_{x,g}$. Thus, the "kink" in 60 Å film in Figure 1 still indicates a departure from the rubbery state expansion.

The complementary beam-PALS results for the fitted o-Ps lifetime τ_{Ps} vs T are presented in Figure 2 for a similar range of PC film thickness, h. For the relatively

Table 1. Compilation of the Apparent T_g's and Expansion Coefficients Obtained by the Various Techniques[a]

SXR	h (Å)	$T_{g,x}$ (°C)	$\beta_{x,g}$ ($\times 10^{-4}$ °C^{-1})	$\beta_{x,r}$ ($\times 10^{-4}$ °C^{-1})
	717	142 ± 9	1.17 ± 0.19	4.37 ± 1.12
	424	135 ± 12	1.01 ± 0.21	4.31 ± 0.60
	252	137 ± 10	0.92 ± 0.22	4.24 ± 0.60
	142	125 ± 6	0.13 ± 0.24	3.74 ± 0.39
	60	102 ± 6	−1.83 ± 0.32	3.73 ± 0.28
PALS	**h (Å)**	**$T_{g,p}$ (°C)**	**$\beta_{p,g}$ ($\times 10^{-4}$ °C^{-1})**	**$\beta_{p,r}$ ($\times 10^{-3}$ °C^{-1})**
	bulk	144.2 ± 1.1	8.38 ± 0.27	3.36 ± 0.12
	1011	146.2 ± 4.7	7.7 ± 0.5	3.13 ± 0.31
	321	144.8 ± 3.3	6.31 ± 0.39	2.83 ± 0.17
	142	134.4 ± 4.1	4.44 ± 0.62	2.13 ± 0.13
	89	138 ± 13	1.6 ± 1.3	1.26 ± 0.27
	75.8	120 ± 15	−1.5 ± 1.8	0.60 ± 0.17
INS	**h (Å)**	**$T_{g,u}$ (°C)**	**$\beta_{u,g}$ ($\times 10^{-3}$ °C^{-1})**	**$\beta_{u,r}$ ($\times 10^{-2}$ °C^{-1})**
	bulk	154.1 ± 2.1	4.70 ± 0.10	2.54 ± 0.15
	1015	159.5 ± 1.3	4.33 ± 0.06	1.04 ± 0.02
	298		3.99 ± 0.09	
	128		2.61 ± 0.13	
	75	217 ± 2	2.26 ± 0.06	1.39 ± 0.08

[a] The errors in β reflect the standard uncertainty in the slopes from the linear fits indicated in Figures 1−3 while the errors in the apparent T_g are the uncertainty in the intersection of the two linear fits (propagation of slope and intercept errors).

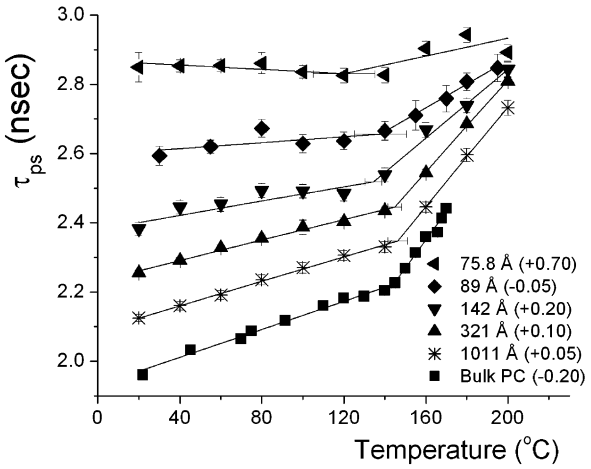

Figure 2. Thermal variations of the orthopositronium lifetimes, τ_{Ps}, as a function of film PC film thickness. The curves are offset vertically for clarity by a constant addition indicated in the legend. The intersection of the fits, indicated by the solid lines, defines the apparent $T_{g,p}$ as described in the text. Standard uncertainties (one standard deviation) in τ_{Ps} are typically the size of the plotting symbol. The bulk PC data are from ref 47.

small range of τ_{Ps} values observed in this work, the proportionality between cavity size (diameter, assuming a spherical cavity) and τ_{Ps} is approximately linear (see ref 6), corresponding to cavities 5−6 Å in diameter. As with the SXR data, each curve is an average of multiple (2−3) heating and/or cooling curves. The error bars indicate the averaged (of multiple runs) standard deviation in the lifetimes from the PFPOSFIT fitting program.[42] Once again, several of the expansion curves are vertically offset by a constant value (indicated in the legend) for clarity. When low implantation energy positrons are used to study ultrathin films, the fast positronium formation creates a shoulder or background in the spectrum in the region corresponding to the time-of-flight of positronium atoms from the sample surface to the surrounding annihilating surface,[45] which in this case is about 8−10 ns. This fast positronium background

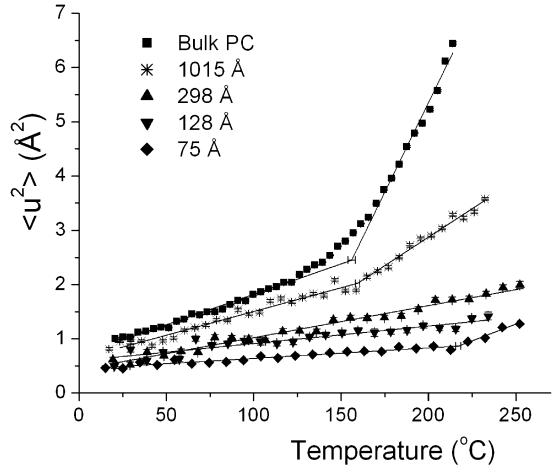

Figure 3. Mean-square atomic displacement $\langle u^2 \rangle$, normalized to zero at −225 °C, as a function of PC film thickness. The solid lines indicate linear fits used to extract the apparent $T_{g,u}$ values. The standard uncertainties (one standard deviation) in $\langle u^2 \rangle$ are indicated by the vertical error bars.

can slightly influence the fit of the 1−3 ns o-Ps component that is of interest here, so we caution that the pore size determined from the fitted τ_{Ps} may not be an absolute determination. However, the variations of τ_{Ps} with T are robust and the emphasis of this work.

In each PC film there is a kink in the thermal variation of τ_{Ps}, similar to the bulk data[46] where the discontinuity coincides with the calorimetric $T_{g,c}$. The lowest set of data points in Figure 2 designated as bulk PC is reproduced from ref 46, in which a thick (several millimeters) PC film was analyzed with bulk-PALS measurement. The same least-squares fitting routine is used to extract the apparent PALS glass transition temperatures, $T_{g,p}$, from the intersection of linear fits above and below the kink for both the thin films and bulk PC. The slopes of these linear fits divided by the lifetime at $T_{g,p}$ similarly define the PALS coefficients of thermal expansion above ($\beta_{p,r}$) and below ($\beta_{p,g}$) $T_{g,p}$. The fitted values of $T_{g,p}$ and the expansion coefficients are presented in Table 1. As with SXR, there is a decrease of $\beta_{p,g}$ with increasing degree of confinement. In the 76 Å film, $\beta_{p,g}$ becomes effectively zero, which is qualitatively in line with the negative value of $\beta_{x,g}$ in the SXR data for the 60 Å film. Unlike the SXR data, there is a statistically significant reduction of $\beta_{p,r}$ in the PALS data with film thinness (a trend also observed for polystyrene in ref 6). The suppressed thermal expansion with smaller h both above and below $T_{g,p}$ makes it increasingly difficult to determine the kink position for $T_{g,\beta}$. Nevertheless, we find a weak decrease in the apparent $T_{g,p}$ (similar to that for the SXR data) with decreasing film thickness.

Figure 3 extends the comparison to incoherent elastic neutron scattering, where $\langle u^2 \rangle$ is plotted as a function temperature and film thickness. In this article we do not present the T and Q dependence of the elastic scattering intensities used to calculate these $\langle u^2 \rangle$ values; these data, for these same PC films, have been discussed in great detail previously.[30,32] Figure 3 shows that at any temperature $\langle u^2 \rangle$ is suppressed as the degree of thin film confinement increases. It should be emphasized that the magnitude of this suppression is significant. Strictly speaking, the model used to calculate $\langle u^2 \rangle$ is based on a 3-D harmonic oscillator while thin films clearly approach 2-D. One could argue that the reduction of $\langle u^2 \rangle$ is an artifact of applying a 3-D model to a 2-D film. However, the suppressions that we observe are too great. At the calorimetric T_g, $\langle u^2 \rangle = 2.4$ Å^2 for bulk PC, which drops to 0.7 Å^2 for the thinnest film. If the reduction were simply due to the loss of one degree of freedom, the thin film value would be $^2/_3$ the bulk, i.e., $\langle u^2 \rangle = 1.6$ Å^2. The suppressions of $\langle u^2 \rangle$ with film thickness are significant.

As with the SXR and PALS data, there is a strong upturn in $\langle u^2 \rangle$ in the region of the bulk T_g, suggesting that a similar apparent T_g assignment can be made. In the bulk, it is well-known that this crossover corresponds to the calorimetric $T_{g,c}$.[47−51] To be consistent with the SXR and PALS data fitting, the same least-squares routine is employed to find the two most appropriate linear fit functions that define an apparent $\langle u^2 \rangle$ glass transitions, $T_{g,u}$. The corresponding linear fits are indicated in Figure 3. In bulk PC, the data between 125 and 165 °C had to be ignored to get the fit to converge. (The data are more smoothly curved than bilinear.) Undoubtedly, the choice of which data points to exclude will affect a systematic error that is much larger than the statistical uncertainty of the bilinear fitting, so the systematic error is chosen and citied in Table 1. Nevertheless, the bulk and 1015 Å films clearly indicate an apparent $T_{g,u}$ that is in nominal agreement with (if not slightly greater than) the bulk calorimetric T_g.

For the thinner films in Figure 3, a clear indication of the apparent $T_{g,u}$ becomes difficult; the curves appear to flatten with decreasing film thickness, and we cannot assign a statistically significant apparent T_g to the 298 and 128 Å films. However, the fitting routine detects a statistically significant kink at 217 °C in the 75 Å film, and we believe that this increase in the anharmonicity of atomic motions is real (whether or not it is related to T_g). Similar measurements on PMMA and PVC thin films reported elsewhere[32] support the notion that the apparent $T_{g,u}$ increases with decreasing film thickness (statistics were greater in these cases), indicating the effect may be general. Returning to the 298 and 128 Å PC films that lack the apparent $T_{g,u}$, notice that the point-to-point variations in $\langle u^2 \rangle$ are greater in comparison to the 75 Å and films. This is because the data collection times were 5 times greater for the 75 Å films, which outweighs the fact that there was roughly half the sample mass. If better statistics were obtained on the 298 and 128 Å films, the apparent $T_{g,u}$ trends with film thickness might be more evident. Regardless of the difficulties in assigning $T_{g,u}$, confinement clearly suppresses $\langle u^2 \rangle$ above and below the 150 °C bulk calorimetric T_g. As with the SXR and PALS data, $\beta_{u,g}$ can be extracted from the slopes of the linear fit. (Where no $T_{g,u}$ is apparent, the entire straight line fit is attributed to the glass.) Table 1 shows that $\beta_{u,g}$ decreases with the level of confinement, in accordance with the trends of $\beta_{x,g}$ and $\beta_{p,g}$. The strong suppression of $\langle u^2 \rangle$ above 150 °C is in qualitative agreement with the PALS $\beta_{p,r}$ but is not reflected in the SXR $\beta_{x,r}$.

Discussion

Specular X-ray Reflectivity. SXR is an established technique to probe confinement effects in thin polymer films.[7−9,23,24] Figure 4 summarizes the apparent T_g from both SXR and PALS measurements. $T_{g,x}$ and $T_{g,p}$ agree both qualitatively and quantitatively and appear to only decrease slightly (about one standard deviation) with decreasing film thickness. For PS films, apparent T_g

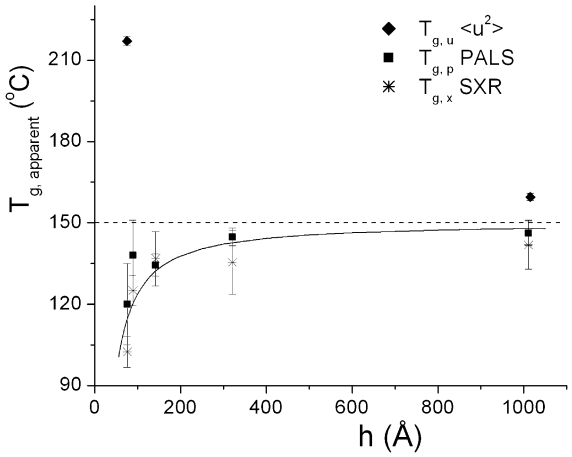

Figure 4. Variations of the apparent T_g estimates ($T_{g,x}$, $T_{g,p}$, and $T_{g,u}$) with film thickness h as determined from SXR, PALS, and INS, respectively. The error bars indicate one standard deviation in identifying the intercept of the two linear functions that identify the apparent T_g in Figures 1−3. The solid line is the fit of eq 3 to the combined SXR and PALS data sets. The dashed line indicates the calorimetric T_g of PC measured by DSC.

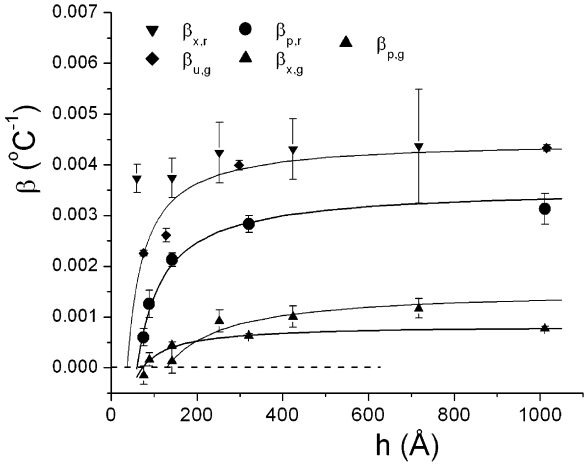

Figure 5. Film thickness (h) variation of the various thermal expansion coefficients (β) as defined in the text. The error bars represent one standard deviation in the slopes from the linear fits in Figures 1−3.

depressions like Figure 4 are sometimes fit with the following empirical expression, inspired by phase transition analogies:

$$T_g(h) = T_g(\infty)\left[1 - \left(\frac{a}{h}\right)^{\gamma}\right] \tag{3}$$

where $T_g(\infty)$ and $T_g(h)$ are the bulk and thin film glass transitions, h is the film thickness, a is a characteristic length scale, and γ is a dimensionless exponent. Setting $T_g(\infty) = T_{g,c} = 150$ °C, the fit of eq 3 to the combined SXR and PALS data sets (indicated by the solid line in Figure 4) yields a crossover length scale of $a = 20$ Å and finite size stretching exponent $\gamma = 1.1$. For similar supported PS films these fit parameters are $a = 32$ Å and $\gamma = 1.1$.[4] Empirically, the similar a's and identical γ's simply imply, to a first approximation, that the deviations occur at similar length scales in PC as compared to PS.

More notable than the modest suppression of the apparent T_g, Table 1 shows a diminished $\beta_{x,g}$ with thin film confinement; the same cannot be said for $\beta_{x,r}$. This is graphically seen in Figure 5 where all the β's are plotted as a function of film thickness. A reduction of $\beta_{x,g}$ occurs for films less than 200 Å thick, a length scale close to the ideal chain dimension of PC under Θ conditions. Using a statistical segment length of 13.4 Å[29] and the molecular mass of the PC used here, the radius of gyration (R_g) is estimated to be 61 Å, or a molecular diameter of 122 Å. We reasonably expect that diminished molecular mobility at the segmental length scales and beyond accompanies this reduced thermal expansion. There have been attempts to quantify this notion of reduced mobility in terms of "layer" models.[6,7,23,24,39] A reduction of β with decreasing film thickness can be simplistically modeled with an immobilized (nonexpanding) layer of constant thickness (δ) near the substrate in conjunction with a layer of variable thickness that has bulklike expansion. One can estimate this "dead layer" thickness δ by extrapolating the results in Figure 5 to $\beta_{x,g} = 0$ where $h = \delta$. We do this quantitatively using the formula

$$\beta_{x,g}^{film} = \beta_{x,g}^{bulk}(1 - \delta/h) \tag{4}$$

where $\beta_{x,g}^{bulk}$ and $\beta_{x,g}^{film}$ are the thermal expansion coefficients of the bulk and thin film, respectively.

Using this "dead layer" approximation for the extent of reduced mobility, we fit $\delta = 130 \pm 20$ Å and $\beta_{x,g}^{bulk} = (1.52 \pm 0.15) \times 10^{-4}$ °C^{-1} from the glassy state SXR data, limiting the fit to the $\beta_{x,g}$ values that are positive. Although the model does not account for the negative $\beta_{x,g}$ in the thinnest film, we can include this point into the fit and find that $\delta = 130 \pm 3$ Å. We stress that using eq 4 does not imply that we literally believe that the confined polymer film can be neatly partitioned into a rigid or nonexpanding layer combined with a bulklike layer. It is highly unlikely that a molecularly thin film can be separated into distinct layers at all. However, eq 4 provides a simple means to quantify the extent of the reduced motion; a larger fitted δ indicates a more dramatic reduction.

The fitted $\beta_{x,g}^{bulk}$ from eq 4 appear reasonable, although it is truly difficult to estimate what the bulk expansion coefficients are from SXR. In the thin film geometry expansion is constrained (prohibited) within the plane of the film. The linear expansion coefficient obtained from volumetric dilatometry ($\beta_{l,g} = 7.13 \times 10^{-5}$ °C^{-1} [52]) needs to be corrected for this lateral constraint using continuum mechanics and Poisson's ratio ν[7] before comparing to the fitted $\beta_{x,g}^{bulk}$. Estimating $\nu = 0.33$ below $T_{g,x}$ yields a laterally constrained bulk expansion coefficient of 1.43×10^{-4} °C^{-1}, which is in accord with the fitted $\beta_{x,g}^{bulk} = (1.52 \pm 0.15) \times 10^{-4}$ °C^{-1}. The agreement between the fitted and estimated β is remarkable given the estimated ν's and the simplistic nature of the dead layer model. A decrease in the apparent T_g is sometimes interpreted as evidence for enhanced mobility. However, the decreasing β gives a contradictory indication for the change of mobility in the confined films. In the ensuing discussions, this apparent contradiction is explored in greater depth.

Positron Annihilation Lifetime Spectroscopy. Like SXR, beam PALS is well established in characterizing glass transitions in thin polymer films.[6,39] Figure 4 shows that the PALS $T_{g,p}$'s are in good agreement with the SXR data and support the notion of a weak decrease in the thin film glass transition temperature with

decreasing thickness. Figure 5 indicates that the PALS β's decrease with decreasing film thickness, in both the glass and the rubbery states. Equation 4 can be used to quantify the reduced mobility through the dead layer thickness, with $\delta = 60 \pm 3$ Å and $\delta = 73 \pm 7$ Å above and below $T_{g,p}$, respectively. The similar values of δ suggest that the extent to which thin film confinement reduces thermal mobility is similar above and below $T_{g,p}$. The PALS δ's are also consistent with the immobilized interface predictions from measurements on PS films.[6] However, in the case of PC films supported on strongly interacting hydrogen-passivated Si substrates,[39] the preferential interactions with the passivated surface lead to a thicker dead layer ($\delta \approx 80-100$ Å) or a greater reduction of mobility. Fits to eq 4 also give an estimation of the bulk expansion coefficients with $\beta_{p,r}^{bulk} = (3.53 \pm 0.17) \times 10^{-3}$ °C^{-1} and $\beta_{p,g}^{bulk} = (8.3 \pm 0.4) \times 10^{-4}$ °C^{-1}. They are in very good agreement with the respective fitted values from the bulk-PALS experiments[46] of $(3.36 \pm 0.12) \times 10^{-3}$ °C^{-1} and $(8.38 \pm 0.27) \times 10^{-4}$ °C^{-1} presented in Table 1.

Notice that the β's from the beam-PALS experiments are significantly larger than their SXR counterparts. For polymers it is well-known that the expansion coefficients from PALS are approximately 1 order of magnitude greater than their corresponding macroscopic values.[53−57] SXR measures film thickness, a continuum property analogous to the macroscopic volume of a bulk sample. The macroscopic thermal expansion is dominated by the weakest bonding in the system, namely, the van der Waals interactions between polymer chains. (The intramolecular covalent bonds are much stronger.) Typically, glassy polymers have macroscopic expansion coefficients on the order of 10^{-4} °C^{-1}, which reflects an average over all intermolecular vibrations. However, the packing inefficiencies or cavities evidenced by PALS experience particularly soft intermolecular potentials; low-density heterogeneities mean a lack of nearest neighbors in the immediate vicinity of the packing defect. These regions produce greater thermal fluctuations than the densely packed regions of the glass, and the local thermal expansion coefficients are thus much greater than the their macroscopic analogues. Typical glassy polymers show PALS expansion coefficients on the order of 10^{-3} °C^{-1}.[53−57] However, since the heterogeneities seen by PALS compose a minor volume fraction of the amorphous polymer, the macroscopic expansion, which averages over both the PALS heterogeneities and the dense domains, is significantly reduced. We will further consider these effects after corresponding the neutron scattering data below.

Incoherent Neutron Scattering. In the preceding discussions, the thermal expansion coefficients from SXR and PALS were used to estimate the extent of reduced thermal mobility in thin PC films. Here INS is invaluable because it directly quantifies the amplitude of the atomic motion in the thin polymer films. Consistent with a zone of reduce mobility near the Si interface, Figure 3 shows a decisive reduction of $\langle u^2 \rangle$ at all T as the PC films become increasingly thin. This isothermal reduction of $\langle u^2 \rangle$ with decreasing film thickness is further illustrated in Figure 6 for several different temperatures; at each temperature $\langle u^2 \rangle$ asymptotically approaches the bulk value with increasing film thickness. Since $\langle u^2 \rangle$ is averaged across the entire film thickness, a dynamically hindered interfacial region of constant thickness is consistent with the observed

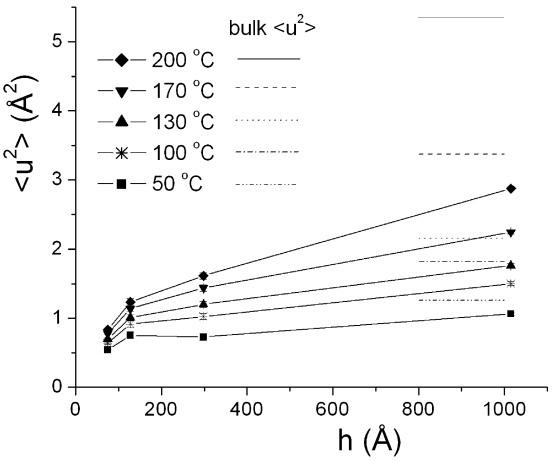

Figure 6. Isothermal variations of $\langle u^2 \rangle$ displayed as a function of film thickness h, both above and below the calorimetric T_g. The short horizontal lines on the right side of the plot indicate the value of $\langle u^2 \rangle$ in bulk PC at each temperature.

reduction of $\langle u^2 \rangle$ with decreasing film thickness. On the contrary, we do not see evidence for enhanced thin film mobility as might be (erroneously) inferred from the suppressed SXR and PALS apparent glass transitions. We elaborate on this important notion below.

Arguments of enhanced mobility near a free surface are often invoked to account for thin film T_g suppressions similar to Figures 1 and 2, based on the supposition that mobility increases as T_g decreases for a fixed T. These arguments are hard to reconcile with the reduction of $\langle u^2 \rangle$, suggesting that a lower T_g does not necessarily imply that the dynamic amplitudes are greater. To better understand how $\langle u^2 \rangle$ relates to mobility, it is useful to examine the frequency dependences of the formalisms used to calculate $\langle u^2 \rangle$ from the full neutron scattering density of states. (Recall that a simple harmonic approximation was employed here.) $\langle u^2 \rangle$ is actually integral over the density of states $g(\omega)$, divided by the frequency ω: $\langle u^2 \rangle \propto \int g(\omega)/\omega \, d\omega$.[58] Given the energy resolution of the spectrometer, this integral starts at 211 MHz and extends well into the high-frequency optic modes. The integral's inverse dependence on the square of the frequency means that the low-frequency motions, which naturally occur with larger amplitudes, dominate $\langle u^2 \rangle$. This is why $\langle u^2 \rangle$ becomes appreciable above T_g; passage into the rubbery state enables low-frequency, large-amplitude motions of the entire chain. It appears that thin film confinement suppresses these larger amplitude motions. Later we will discuss correlations between $\langle u^2 \rangle$ and viscosity (another macroscopic indicator of mobility). We also note that the low-frequency bias of $\langle u^2 \rangle$ would be more sensitive to a surface layer with fluidlike motions (low frequency, large amplitude) than a buried interface of suppressed dynamics (high frequency, small amplitude). We do not see evidence for a surface layer of enhanced mobility.

This message of reduced mobility from the INS measurements is restated with the $\langle u^2 \rangle$ expansion coefficient β_u. This is shown in Figure 5 where the β below the $\langle u^2 \rangle$ kink ($\beta_{u,g}$) is compared to $\beta_{x,g}$ and $\beta_{p,g}$ Notice that we do not report $\beta_{u,r}$ for some of the intermediate thin films because of the difficulties in establishing the $\langle u^2 \rangle$ kink mentioned earlier. Figure 5 illustrates that all three experimental techniques indicate a reduction of β with confinement. If the dead layer

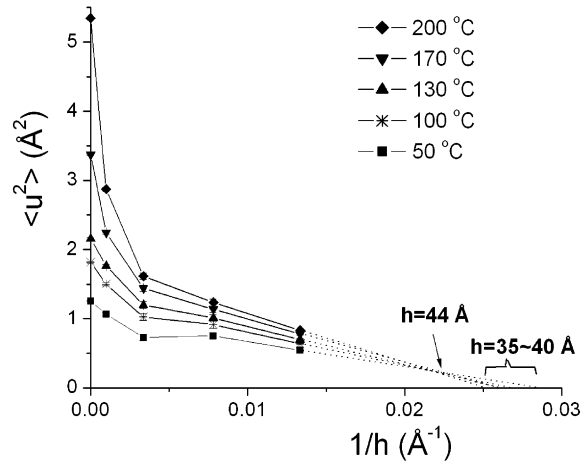

Figure 7. Isothermal variations of $\langle u^2 \rangle$ displayed as a function of inverse film thickness $1/h$. The linear function defined by the last two data points at each temperature is extrapolated to smaller $1/h$ values as indicated by the dashed lines. Notice that the extrapolations cross over near $h \approx 44$ Å and then fan out across the x-axis in the range of $h \approx 35-40$ Å.

model is used to estimate extent of the dynamic suppression, eq 4 yields $\delta = 38 \pm 4$ Å and $\beta_{u,g}^{bulk} = (4.48 \pm 0.18) \times 10^{-3}$ °C^{-1}. The fitted $\beta_{u,g}^{bulk}$ is consistent with the experimentally measured value of $(4.70 \pm 0.10) \times 10^{-3}$ °C^{-1}, reported in Table 1. The δ derived from the $\langle u^2 \rangle$ is not in agreement to within statistical uncertainty with the SXR and PALS values, but they are in accord to within an order of magnitude. This is probably reasonable given the simplistic nature of the dead layer model.

Without a sufficient set of $\beta_{u,r}$ data, we cannot apply the dead layer model to the INS data above T_g. However, we can approximate a somewhat comparable thickness of the reduced mobility layer in Figure 7 where the isothermal $\langle u^2 \rangle$ variations are plotted as a function of inverse film thickness. Notice that if we crudely extend the linear trend established by the two thinnest data points, the extrapolated values for the different T cross over at $h \approx 44$ Å. In the dead layer model, δ does not change with T. The crossover at which all the $\langle u^2 \rangle$ become equal is therefore in the spirit of a dead layer thickness and correspondingly comparable to $\delta = 38 \pm 4$ Å for the glassy state data. Furthermore, when these linear extrapolations are extended to the actual point where $\langle u^2 \rangle = 0$, they cross the x-axis over a range of thickness from approximately 35 to 40 Å. This zero mobility estimate, while crude, is also consistent with the preceding dead layer estimates.

It is notable that $\beta_{u,g}$ and $\beta_{p,g}$ in Figure 5 are similar in their order of magnitude, both considerably greater than $\beta_{x,g}$. Previously, we argued that a larger $\beta_{p,g}$ in comparison to $\beta_{x,g}$ is because PALS is primarily sensitive to the low electron density heterogeneities, regions with very soft intermolecular potentials and enhanced thermal fluctuations. It is therefore interesting that the thermal fluctuations of $\langle u^2 \rangle$ more closely resemble the PALS nanopore expansion, suggesting they probe similar regions. This turns out to be reasonable since there are several correlations between the PALS nanopores and $\langle u^2 \rangle$.[51,55,59,60] That $\beta_{p,g}$ and $\beta_{u,g}$ have similar magnitudes provides further evidence that the two techniques probe similar or related quantities. The physical picture that arises from this discussion is that $\langle u^2 \rangle$ reflects heterogeneous dynamics, localized to the low-density regions sensed by PALS. Naturally, these regions are where the largest amplitude and lowest frequency motions that naturally dominate $\langle u^2 \rangle$ would flourish, not in the densely packed domains of the glass.

The decrease of $\langle u^2 \rangle$ with confinement then implies that the density heterogeneities are suppressed as the films become thinner, i.e., molecules become more strongly and uniformly caged by their neighbors. This would be consistent with the reduced thermal expansion coefficients. One would also expect then a reduction of the so-called "free volume" with decreasing film thickness. In fact, molecular dynamics simulations[61] on confined fluids suggest that such a mechanism is operative. In this respect, beam PALS might be viewed as the ideal "free volume" probe. Unfortunately though, complications prevent us from addressing this issue adequately. There is a significant reduction in the intensity of the relative fraction of o-Ps annihilation events (relative to the free positron and parapositronium annihilation events) from a bulklike value of 34% in the 1011 Å film to 7% in the highly confined 76 Å film. The fewer o-Ps annihilation events could be interpreted as reduced heterogeneities in the confined film (fewer PALS defects). However, thinner films also require lower positron implantation energies, which reduce the number of spur electrons. This "spur" is a cloud of electrons that the high-energy incident positron knocks free from their orbitals in the polymer. o-Ps forms (and annihilates) when the positron localizes and combines with one of these spur electrons. The reduced relative number of o-Ps annihilation events may simply reflect the smaller number of spur electrons created in the thin films at smaller implantation energies.[38] Unfortunately, we cannot exclude this explanation for the reduced o-Ps annihilation intensity in these confined films; it is unclear whether the reduced o-Ps annihilation intensities are due to reduced heterogeneity.

While SXR and beam PALS are well-documented techniques for characterizing the glass transition shifts in thin polymer films, these are some of the first data[30] where INS has been used to study confinement effects in thin polymer films (see also refs 31−33). Whereas T_g-like features are seen in the bulk and 1015 Å films, it is remarkable that in the regions of $T_{g,x}$ and $T_{g,p}$ similar features in $\langle u^2 \rangle$ are not seen for films thinner than approximately 1000 Å. This might be is an issue of sensitivity. The $\langle u^2 \rangle$ data from the thin films is signal limited (1−10 mg of PC whereas 200 mg would be ideal), and it is plausible that features in $\langle u^2 \rangle$ near $T_{g,x}$ or $T_{g,p}$ are simply masked by experimental noise. We see a statistically significant transition at 217 °C in the thinnest (76 Å) films, but this is considerably higher than the conventional calorimetric T_g of PC; 217 °C is 1.2 times the bulk calorimetric T_g and also nominally consistent with the melting temperature of crystalline PC (making no implications about thin film crystallinity with this statement). In this respect, the high-T kink may not even be related to the conventional bulk glass transition. The possibility of multiple transitions is discussed briefly below. Nevertheless, we include these data on the apparent T_g plot in Figure 4.

Comparison of the Constrained "Dead" Layer Estimates. Throughout this discussion we have estimated the extent of reduced mobility in terms of the dead layer model. To summarize, Table 2 compares the δ values from the various techniques. PALS and INS result in similar δ's (on the order of 40−70 Å), consistent with the fact that both techniques are primarily sensi-

Table 2. Summary of the Fit Parameters for the Dead Layer Analysis Using Eq 4

	δ_g (Å)	δ_r (Å)	β_g^{bulk} (°C^{-1})	β_r^{bulk} (°C^{-1})
SXR	130 ± 20		$(1.52 \pm 0.15) \times 10^{-4}$	
PALS	73 ± 7	60 ± 3	$(8.3 \pm 0.4) \times 10^{-4}$	$(3.53 \pm 0.17) \times 10^{-3}$
INS	38 ± 4		$(4.48 \pm 0.18) \times 10^{-3}$	

tive to the structurally open regions that display larger amplitude motions. However, there does not appear to be agreement with the dead layer thickness values predicted by the SXR data. The SXR δ in the glassy state is considerably larger (130 Å) than the PALS and INS estimates, while the SXR rubbery state does not show a statistically significant reduction of mobility.

A reduced dead layer thickness from SXR might be anticipated given that PALS and INS are most sensitive to the soft, heterogeneous regions where local motions are extensive. Both PALS and INS are sensitive to local segmental motions, such as rotations and/or librations of the phenyl rings, methyl groups, etc. These local motions provide less in terms of the macroscopic mobility/expansion that is reflected in SXR, for the same reason why the β's from PALS and INS are an order of magnitude greater than SXR. Therefore, reduction of the local segmental motion upon confinement would more significantly impact PALS and INS data in comparison to the SXR. This could explain lack of reduced mobility in the SXR data above $T_{g,x}$. However, this explanation is inconsistent with the largest δ evidenced in the SXR glassy state regime. To this failure, we stress that the dead layer model does not contain the proper physics to explain the negative β the thinnest film in the glassy state SXR data. Clearly, the thermal response in this regime is complicated, and there are other mechanisms operative in this regime (see accompanying paper for further discussion on this topic).

Another shortcomings of the dead layer model is that it does not describe the decrease of $T_{g,x}$ and $T_{g,p}$ with film thickness. In the past this has been resolved by incorporating a thin (few nanometers) surface layer of highly mobile polymer, i.e., a three-layer model.[3,6] A surface layer of enhanced mobility could explain the apparent discrepancy between the decreased $T_{g,x}$ and $T_{g,p}$ and the ubiquitous decrease of β. In principle, it makes intuitive sense that segments near the free surface should have enhanced mobility. Recently, we provided experimental evidence[62] that the molecules at a free surface of glassy PS can relax faster than those in the bulk. However, it is hard to believe that a sub-100 Å polymer film, thinner than the unperturbed dimensions of the macromolecule, can be neatly divided into immobilized, bulklike, and fluidized layers. This is especially true in bulk PC where the sub-T_g molecular motions have an in-chain cooperativity that extends for approximately 7−9 repeat units, or roughly 90−120 Å.[63−65] An immobilized layer near the substrate would seemingly influence the dynamics near the free surface (and vice versa) due to the strong interaction coupling. Furthermore, the estimated dead layer can be comparable (or even greater) than the entire film thickness in the thinnest films that show suppressions of $T_{g,x}$ and $T_{g,p}$. It is then somewhat arbitrary to reassign a portion of the dead layer to be extremely mobile.

Reduced Thin Film Mobility. In the Introduction we described how the glass transition is often defined by a kink in the temperature dependence of a thermophysical parameter, such as density, film thickness, etc., and that reduction in the glass transition as a function of film thickness is sometime used to infer an increase in the overall molecular mobility. However, we find in the present work that such an inference may not always be appropriate or meaningful. While SXR and PALS indicate a reduced glass transition temperature, the β's and requisite dead layers from all three techniques indicate hindered mobility. Consistent with this picture, the average mean-square atomic displacements are reduced as the film thickness decreases; one must heat to higher temperature to induce large-scale displacements. We acknowledge that in bulk glasses there are good correlations between an enhanced level of anharmonicity in $\langle u^2 \rangle$ and T_g[47−51] but that in thin films studied here these quantities appear to be anticorrelated. Moreover, the relationship between $\langle u^2 \rangle$ and T_g is not understood. Recent reviews[48,66] cite this as one of the remaining unexplained phenomena of glass formation. The time scales implicit in $\langle u^2 \rangle$ and more traditional measures of T_g differ by at least 9−10 orders of magnitude. $\langle u^2 \rangle$ clearly reflects local atomic motion while T_g involve large-scale, cooperative rearrangements of atoms/molecules. It is possible that thin film confinement curtails the level of cooperativity at the glass transition, meaning that lower temperatures are required to fully activate the motion. However, the interatomic potentials could still be stiffened meaning that mobility is reduced. In this respect, $\langle u^2 \rangle$ should not be interpreted in terms of a glass transition, per se. Rather, $\langle u^2 \rangle$ is a reflection of the high-frequency atomic/molecular mobility.

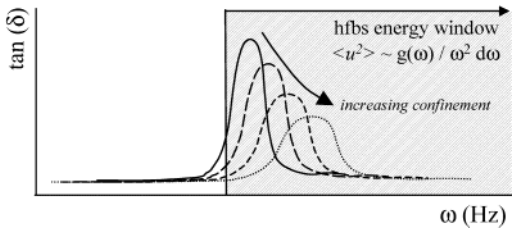

Figure 8. A cartoon depicting how the frequency behavior of the α-relaxation changes with confinement, based on experimental dielectric measurements of salol in a controlled pore glass.[67] If the energy resolution of the HFBS spectrometer is as indicated with respect to the α-relaxation, the frequency weighting of the integral will lead to a reduction of $\langle u^2 \rangle$ with increasing confinement.

Nevertheless, the observation that the apparent T_g by SXR and PALS decreases, while the amplitude of $\langle u^2 \rangle$ also decreases, with increasing film thinness is still somewhat discerning. This is perhaps more distressing when comparing to recent simulation data for a polymer fluid confined between parallel plates with unfavorable interactions between the polymer and the rigid surfaces.[20] These simulations show that T_g decreases with decreasing film thickness, accompanied by an increase, not decrease, of $\langle u^2 \rangle$. To help alleviate this concern, we speculate on the origin of this apparent paradox below. We do not doubt the validity of the simulation data[20] but further point to supporting experimental dielectric data. Kremer's group studied salol in controlled pore glasses[67] and found that the α-relaxation broadens and shifts to shorter relaxation times (higher frequency) with increasing confinement, while at the same time the calorimetric T_g decreases. This trend for the α-relaxation is schematically depicted in the cartoon of Figure 8. Recall that the integral to determine $\langle u^2 \rangle$ from the

vibrational density of states contains the $1/\omega$ weighting; low-frequency motions contribute significantly more to $\langle u^2 \rangle$ than high-frequency motions. If the energy resolution of the spectrometer relative to shifting of the α-relaxation peak were as indicated in the cartoon of Figure 8, one could easily envision the reduction $\langle u^2 \rangle$ with increasing confinement; the α-relaxation moves into a regime of the integral where the motions are weighted less, leading to a smaller $\langle u^2 \rangle$.

Unfortunately, we do not have dielectric or other dynamic data to track the frequency of the α-relaxation as a function of confinement as in the case of salol. The full inelastic neutron scattering spectra contain this information, but our films are so thin that we can only resolve the Q dependence of the elastic peaks. However, there are comparable neutron scattering measurements by Zorn and co-workers[68] on the same salol system confined to the controlled pore glasses. Like the dielectric data these measurements show that the shifting of the α-relaxation to higher frequency with confinement is accompanied by a strong reduction of the low-frequency modes (below the so-called Boson peak) that the HFBS spectrometer is most sensitive to. Although they do not report mean-square displacement values in their paper, careful examination of the spectra reveals that $\langle u^2 \rangle$ would be reduced with confinement. This suggests that the T_g shift to lower temperature is consistent with the reduction of $\langle u^2 \rangle$. In two succeeding articles, several of the same authors in fact do confirm a decrease of $\langle u^2 \rangle$ with increasing confinement in both polymers (poly(dimethylsiloxane) and poly(propylene glycol))[69] and toluene[70] inside controlled pore glasses. These observations suggest that confinement suppresses the lower frequency modes. The result is a shift to higher frequency, but smaller amplitude, motions. We interpret this as reduced mobility because things like thermal expansion, diffusion, transport, etc., will be suppressed. Upon cooling, the more localized and faster motions of the glass will also remain in equilibrium to lower temperatures, which is consistent with the reduced calorimetric T_g, but it is important to realize that the length scale of the motion has been reduced.

Consistent with the notion of reduced mobility in these thin films, there are empirical correlations between viscosity η and $\langle u^2 \rangle$. A $\eta \propto \exp(1/\langle u^2 \rangle)$ dependence has been seen by Buchenau[71] in Se and Kanaya[72] in polybutadiene. This qualitatively points to enhanced viscosity these confined PC films. This is also consistent with surface forces apparatus measurements by Granick and co-workers that show enhanced viscosity and increased stiffness in confined liquid films, regardless of the interactions with the substrate (attractive or repulsive).[68−70] More directly, we demonstrate a similar thin film confinement induced reduction of $\langle u^2 \rangle$ in thin photoresist films[33] and independently correlate the suppression of $\langle u^2 \rangle$ with reduced photoacid mobility.[76] This is also generally consistent with reduced chain diffusion in thin polymer films.[77−79] Therefore, it is dangerous to infer the dynamical implications of confinement from estimates of crossover or kink temperatures in thermodynamic properties as seen in Figures 1−3. For some reason we observe multiple kinks using the different techniques, raising questions about which characteristic temperature is best identified as the glass transition. The "wrong" choice could potentially lead to erroneous conclusions regarding technologically important issues.

Possibility of Multiple Characteristic Temperatures? The data above reveal apparent T_g's that have qualitatively different dependencies on film thickness. The property specific nature of these transition temperature shifts in thin polymer films is clearly a matter of concern. Is there any sense to these trends? In the following, we discuss the possibility that the signature of the glass transition is changed rather significantly in these thin films. It is worth emphasizing that T_g shifts are normally inferred from changes in a thermodynamic property measurements (specific heat, thermal expansion, etc.) performed under nonequilibrium conditions. A frequency or time scale is always implicit in these measurements, dependent upon the rate at which the property is probed. It seems likely the time scales over which a polymer equilibrates could be quite different in thin films as compared to the bulk and that these changes could be property specific and dependent on the frequency scale of the measurement. Therefore, we must be careful when relating the kink in various thermodynamic properties as a function of T to the glass transition; the phenomenology of the glass transition may need to be entirely reconsidered for the case of supported thin films.

The glass transition is not a thermodynamic phase transition and polymers exhibit a multiplicity of transitional temperatures, even in the bulk. In particular, a variety of properties in "fragile" (rapidly varying viscosity with temperature near $T_{g,c}$) liquids exhibit several changes at an upper transitional temperature which is commonly near $1.2T_{g,c}$. These changes include, but are not limited to, deviations from both the Stokes−Einstein (diffusion and viscosity) and Debye−Einstein (reorientation time and viscosity) relationships,[80−82] a bifurcation of the α and β relaxation processes,[80,83,84] the breaking of ergodicity as predicted by mode coupling theory,[85] and a crossover between the two Vogel−Fulcher relations commonly needed to fit relaxation data above $T_{g,c}$.[86−88] Clearly there is ample evidence for a characteristic temperature near $1.2T_{g,c}$ in glasses considered "fragile", and PC (as many other polymers) are notably considered classic examples of fragile glass formers. We also point out that both poly(methyl methacrylate) and poly(vinyl chloride) display pronounced kinks in $\langle u^2 \rangle$ at $1.2T_{g,c}$ when they are confined to sub-R_g thick films on Si substrates.[32]

It may be relevant that the $\langle u^2 \rangle$ crossover at $T_{g,u}$ approaches $1.2T_{g,c}$ in the highly confined (75 Å) films. Systematic SXR and beam-PALS studies in the vicinity of $1.2T_{g,c}$ have yet to be completed, and it remains to be seen whether similar crossover is observed by the other techniques. We note that a rollover or plateau in τ_{Ps} has also been observed above 200 °C in previous bulk and thin films PALS measurements of PC,[89] nominally consistent with the $1.2T_{g,c}$ mark ($1.2T_{g,c}$ = 217 °C). Likewise, we have confirmed a similar rollover near 210 °C in one of our 100 Å PC film and are in the process of studying the thickness dependence of this phenomenon. Although it was not reported in the original publication,[6] a similar high-temperature rollover was encountered in bulk PS and its thin films.[89] The τ_{Ps} rollover is believed to occur when the fluctuation of the polymer become comparable to the τ_{Ps} lifetimes of a few nanoseconds; i.e., the cavities seen by PALS are not static. This nanosecond time scale is consistent with the 200 MHz resolution of the HFBS spectrometer, making the correlation to $\langle u^2 \rangle$ apparent. At the time, the relevance of

this was not appreciated so we did not study the thickness dependence of these rollover temperatures. Now it would be interesting to see whether this characteristic temperature is affected by thin film confinement. Additionally, the SXR measurements do not extend to $1.2T_c$ because of instrumental limitations. It would also be of interest to circumvent these limitations and see whether a higher temperature transition is observed in the SXR data.

There is also evidence for another characteristic T below $T_{g,c}$ in the viscosity and relaxation times (stress, dielectric, etc.) of bulk supercooled liquids and glasses. Upon extrapolation such properties diverge in accordance with the Vogel−Fulcher−Tamann relation $\eta = \eta_0 \exp(D/T - T_0)$, where η is the viscosity (or other time-dependent property), D and η_0 are constants, and T_0 is the VFT temperature at which the viscosity diverges. Typical estimates of T_0 are $(^2/_3{-}^3/_4)T_{g,c}$. Such a crossover is also seen in thermodynamic calculations of the configurational entropy S_c. Upon cooling an equilibrium liquid S_c begins to drop precipitously near $T_{g,c}$, approaching a plateau at the Kauzmann temperature T_k (typically $T_k \approx T_0$). The thermal fluctuations in S_c become quite large near $T_{g,c}$, giving rise to a specific heat maximum and thus the calorimetric glass transition. In bulk PC, various estimates (from different types of relaxation data) place T_0 between 67 and 102 °C,[90] nominally consistent with the $T_{g,x}$ and $T_{g,p}$ in the highly confined films.

We suggest that the SXR, PALS, and INS measurements become more sensitive to these different crossover temperatures in thin films in a manner that is property specific. If this is true, then the downward shifts of $T_{g,x}$ and $T_{g,p}$ and the increase of $T_{g,u}$ might be rationally interpreted as a crossing over to T_0 (or T_k) and the high-temperature critical temperature $T_c \approx 1.2T_{g,c}$ in the highly confined polymer films. The result is a "broadened" transitional regime in the temperature dependence of the glass transition of the exceeding thin polymer films, a notion that is qualitatively consistent with the recent observations of Kanawa and Jones.[4]

Conclusions

The thermophysical behavior of thin PC films supported on silicon oxide substrates is studied with SXR, PALS, and INS. While SXR and PALS are widely used to characterize the glass transition in thin polymer films, these data represent the first INS measurements on confined polymer films.[29] As the film thickness drops below 200 Å, SXR and PALS indicate a reduction of the polymer's apparent T_g while INS does not, possibly even indicating a T_g increase for this property. To a first approximation, suppressed T_g's are typically cited as evidence for enhanced molecular mobility in thin, confined films. However, all three techniques indicate a general suppression of the thermal mobility in PC for films thinner than approximately 200 Å, the same length scale as the apparent T_g deviations. This reduced mobility is inferred from a decrease in the thermal expansion coefficient defined by SXR (measuring film thickness), PALS (quantifying the nanometer sized density heterogeneities), and INS (characterizing the mean-square atomic displacement $\langle u^2 \rangle$). The extent of the reduced mobility is quantitatively estimated from a simple bilayer model that combines a nonexpanding interfacial layer near the rigid substrate with a layer of bulk like expansion. Estimates of the "dead" interfacial layer range approximately from 42 to 130 Å. More directly, the INS measurements show decisive reductions of $\langle u^2 \rangle$ with decreasing PC film thickness, demonstrating that molecular/atomic motion is curtailed in thin PC films.

Acknowledgment. D.W.G. and H.P. acknowledge their NSF financial support (Grant ECS-9732804) while C.L.S. is grateful for support through a NIST NRC Postdoctoral Fellowship. Additional thanks goes to the NIST Center for Neutron Research for access to their facilities. Furthermore, the authors appreciate the many useful discussions with Albert F. Yee, Robert M. Dimeo, and Eric K. Lin.

References and Notes

(1) Keddie, J. L.; Jones, R. A. L.; Cory, R. A. *Europhys. Lett.* **1994**, *27*, 59.
(2) Keddie, J. L.; Jones, R. A. L.; Cory, R. A. *Faraday Discuss.* **1994**, *98*, 219.
(3) Forrest, J. A.; Dalnoki-Veress, K.; Dutcher, J. R. *Phys. Rev. E* **1997**, *56*, 5705.
(4) Kawana, S.; Jones, R. A. L. *Phys. Rev. E* **2000**, *63*, 021501.
(5) Forrest, J. A.; Dalnoki-Veress, K.; Dutcher, J. R. *Phys. Rev. E* **1998**, *58*, 6109.
(6) DeMaggio, G. B.; Frieze, W. E.; Gidley, D. W.; Zhu, M.; Hristov, H. A.; Yee, A. F. *Phys. Rev. Lett.* **1997**, *78*, 1524.
(7) Wallace, W. E.; Van Zanten, J. H.; Wu, W.-l. *Phys. Rev. E* **1995**, *52*, R3329.
(8) Fryer, D. S.; Peters, R. D.; Kim, E. J.; Tomaszewiski, J. E.; de Pablo, J. J.; Nealey, P. F.; White, C. C.; Wu, W.-l. *Macromolecules* **2001**, *34*, 5627.
(9) Tsui, O. K. C.; Russell, T. P.; Hawker, C. J. *Macromolecules* **2001**, *34*, 5535.
(10) Fukao, K.; Miyamoto, Y. *Phys. Rev. E* **2000**, *61*, 1743.
(11) Fukao, K.; Miyamoto, Y. *Europhys. Lett.* **1999**, *46*, 649.
(12) Fryer, D. S.; Nealey, P. F.; de Pablo, J. J. *Macromolecules* **2000**, *33*, 6439.
(13) Satomi, N.; Takahara, A.; Kajiyama, T. *Macromolecules* **1999**, *32*, 4474.
(14) Ge, S.; Pu, Y.; Zhang, W.; Rafailovich, M.; Sokolov, J.; Buenviaje, C.; Buckmaster, R.; Overney, R. M. *Phys. Rev. Lett.* **2000**, *85*, 2340.
(15) Dinelli, F.; Buenviaje, C.; Overney, R. M. *J. Chem. Phys.* **2000**, *113*, 2043.
(16) Dalnoki-Veress, K.; Forrest, J. A.; Murray, C.; Gigault, C.; Dutcher, J. R. *Phys. Rev. E* **2001**, *63*, 031801.
(17) Grohens, Y.; Brogly, M.; Labbe, C.; David, M.-O.; Schultz, J. *Langmuir* **1998**, *14*, 2929.
(18) Torres, J. A.; Nealey, P. F.; de Pablo, J. J. *Phys. Rev. Lett.* **2000**, *85*, 3221.
(19) Starr, F. W.; Schroder, T. B.; Glotzer, S. C. *Macromolecules* **2002**, *35*, 4481.
(20) Binder, K.; Baschnagel, J.; Paul, W. *Prog. Polym. Sci.* **2003**, *28*, 115.
(21) Forrest, J. A.; Dalnoki-Veress, K.; Stevens, J. R.; Dutcher, J. R. *Phys. Rev. Lett.* **1996**, *77*, 2002.
(22) Forrest, J. A.; Dalnoki-Veress, K.; Stevens, J. R.; Dutcher, J. R. *Phys. Rev. Lett.* **1996**, *77*, 4108.
(23) Pochan, D. J.; Lin, E. K.; Satija, S. K.; Wu, W.-l. *Macromolecules* **2001**, *34*, 3041.
(24) Van Zanten, J. H.; Wallace, W. E.; Wu, W.-l. *Phys. Rev. E* **1996**, *53*, R2053.
(25) Wu, W.-l.; van Zanten, J. H.; Orts, W. J. *Macromolecules* **1995**, *28*, 771.
(26) Graessley, W. W.; Edwards, S. F. *Polymer* **1981**, *22*, 1329.
(27) Wu, S. *J. Polym. Sci., Polym. Phys. Ed.* **1989**, *27*, 723.
(28) Prevorsek, D. C.; De Bona, B. T. *J. Macromol. Sci., Phys.* **1981**, *B19*, 605.
(29) Prevorsek, D. C.; De Bona, B. T. *J. Macromol. Sci., Phys.* **1986**, *B25*, 515.
(30) Soles, C. L.; Douglas, J. F.; Wu, W.-l.; Dimeo, R. M. *Phys. Rev. Lett.* **2002**, *88*, 037401.
(31) Soles, C. L.; Lin, E. K.; Lenhart, J. L.; Jones, R. L.; Wu, W.-l.; Goldfarb, D. L.; Angelopoulos, M. *J. Vac. Sci. Technol. B* **2001**, *19*, 2690.
(32) Soles, C. L.; Douglas, J. F.; Wu, W.-l.; Dimeo, R. M. *Macromolecules* **2003**, *36*, 373.

(33) Soles, C. L.; Douglas, J. F.; Lin, E. K.; Lenhart, J. L.; Jones, R. L.; Wu, W.-l.; Goldfarb, D. L.; Angelopoulos, M. *J. Appl. Phys.* **2003**, *93*, 1978.
(34) Certain commercial equipment and materials are identified in this paper in order to specify adequately the experimental procedure. In no case does such identification imply recommendation by the National Institute of Standards and Technology nor does it imply the material or equipment identified is necessarily the best available for this purpose.
(35) Anker, J. F.; Majkrzak, C. J. In *Neutron Optical Devices and Applications*, SPIE Proceedings 1738; SPIE: Bellingham, WA, 1992; p 260.
(36) Jean, Y. C. In *Positron and Positronium Chemistry*; Schrader, D. M., Jean, Y. C., Ed.; Elsevier: Amsterdam, 1988.
(37) Pethrick, R. A. *Prog. Polym. Sci.* **1997**, *22*, 1.
(38) Xie, L.; DeMaggio, G. B.; Freize, W. E.; DeVries, J.; Gidley, D. W.; Hristov, H. A.; Yee, A. F. *Phys. Rev. Lett.* **1995**, *74*, 4947.
(39) Gidley, D. W.; DeMaggio, G. B.; Frieze, W. E.; Zhu, M.; Hristov, H. A.; Yee, A. F. *Mater. Sci. Forum* **1997**, *255*−*257*, 635.
(40) Sun, J.-N.; Gidley, D. W.; Dull, T. L.; Frieze, W. E.; Yee, A. F.; Ryan, E. T.; Lin, S.; Wetzel, J. *J. Appl. Phys.* **2001**, *89*, 5138.
(41) Schultz, P. J.; Lynn, K. G. *Rev. Mod. Phys.* **1989**, *60*, 701.
(42) Puff, W. *Comput. Phys. Commun.* **1983**, *30*, 359.
(43) Gehring, P. M.; Neumann, D. A. *Phys. B* **1998**, *241*−*243*, 64.
(44) According to ISO 31-8, the term "molecular weight" has been replaced by "relative molecular mass", symbol M_r. Thus, if this nomenclature and notation were to be followed in this publication, one would write $M_{r,w}$ instead of the historically conventional M_w for the mass-average molecular weight, with similar changes for M_n, M_z, and M_v, and it would be called the "mass average relative molecular mass". The conventional notation, rather than the ISO notation, has been employed for this publication.
(45) Gidley, D. W.; McKinsey, D. N.; Zitzewitz, P. W. *J. Appl. Phys.* **1995**, *78*, 1406.
(46) Lie, X. Ph.D. Thesis, The University of Michigan, 1995.
(47) Frick, B.; Richter, D. *Science* **1995**, *267*, 1939.
(48) Angell, C. A.; Ngai, K. L.; McKenna, G. B.; McMillan, P. F.; Martin, S. W. *J. Appl. Phys.* **2000**, *88*, 3113.
(49) Angell, C. A. *Science* **1995**, *267*, 1924.
(50) Colemenero, J.; Arbe, A. *Phys. Rev. B* **1998**, *57*, 13508.
(51) Ngai, K. L.; Bao, L.-R.; Yee, A. F.; Soles, C. L. *Phys. Rev. Lett.* **2001**, *87*, 215901.
(52) Zoller, P. *Standard Pressure*−*Temperature*−*Volume Data for Polymers;* Techomic Pub. Co.: Lancaster, PA, 1995.
(53) Kobayashi, Y.; Zheng, W.; Meyer, E.; McGervy, J. D.; Jamieson, A. M.; Simha, R. *Macromolecules* **1989**, *22*, 2302.
(54) Deng, Q.; Sundar, C. S.; Jean, Y. C. *J. Phys. Chem.* **1992**, *96*, 492.
(55) Bartos, J.; Bandzuch, P.; Sausa, O.; Kristiakova, K.; Kristiak, J.; Kanaya, T.; Jenninger, W. *Macromolecules* **1997**, *30*, 6906.
(56) Soles, C. L.; Chang, F. T.; Bolan, B. A.; Hristov, H. A.; Gidley, D. W.; Yee, A. F. *J. Polym. Sci., Part B: Polym. Phys.* **1998**, *36*, 3035.
(57) Hristov, H. A.; Bolan, B. A.; Yee, A. F.; Xie, L.; Gidley, D. W. *Macromolecules* **1996**, *29*, 8507.
(58) Squires, G. L. *Introduction to the Theory of Thermal Neutron Scattering;* Cambridge University Press: Cambridge, 1978; p 48.
(59) Mermet, A.; Duval, E.; Surovstev, N.; Jala, J. F.; Dianoux, A.; Yee, A. F. *Europhys. Lett.* **1997**, *38*, 515.
(60) Novikov, V. N.; Sokolov, A. P.; Strube, B.; Surovstev, N.; Duval, E.; Mermet, A. *J. Chem. Phys.* **1997**, *107*, 1057.
(61) Gao, J.; Luedtke, W. D.; Landman, U. *Trib. Lett.* **2000**, *9*, 3.
(62) Wallace, W. E.; Fischer, D. A.; Efimenko, K.; Wu, W.-l.; Genzer, J. *Macromolecules* **2001**, *34*, 5081.
(63) Jho, J. Y.; Yee, A. F. *Macromolecules* **1991**, *24*, 1590, 1905.
(64) Xiao, C. Ph.D. Thesis, The University of Michigan, 1991.
(65) Xiao, C.; Jho, J. Y.; Yee, A. F. *Macromolecules* **1994**, *27*, 2761.
(66) Angell, C. A. *J. Phys.: Condens. Matter* **2000**, *12*, 6436.
(67) Arndt, M.; Stannarius, R.; Groothues, H.; Hempel, E.; Kremer, F. *Phys. Rev. Lett.* **1997**, *79*, 2077.
(68) Zorn, R.; Hartmann, L.; Frick, B.; Richter, D.; Kremer, F. *J. Non-Cryst. Solids* **2002**, *307*−*310*, 547.
(69) Schonhals, A.; Goering, H.; Schick, Ch.; Frick, B.; Zorn, R. *Eur. Phys. J. E* **2003**, *12*, 173.
(70) Alba-Simionesco, C.; Dosseh, G.; Dumont, E.; Frick, B.; Geil, B.; Morineau, D.; Teboul, V.; Xia, Y. *Eur. Phys. J. E* **2003**, *12*, 19.
(71) Buchenau, U.; Zorn, R. *Europhys. Lett.* **1992**, *18*, 523.
(72) Kanaya, T.; Tsukushi, T.; Kaji, K.; Bartos, J.; Kristiak, J. *Phys. Rev. E* **1999**, *60*, 1906.
(73) Granick, S. *Science* **1991**, *253*, 1374.
(74) Hu, H.-W.; Granick, S. *Science* **1992**, *258*, 1339.
(75) Demirel, A. L.; Granick, S. *Phys. Rev. Lett.* **1996**, *77*, 2261.
(76) Soles, C. L.; Jones, R. L.; Lenhart, J. L.; Prabhu, V. M.; Wu, W.-l.; Lin, E. K.; Goldfarb, D. L.; Angelopoulos, M. *Proc. SPIE* **2003**, *5039*, 366.
(77) Frank, B.; Gast, A. P.; Russell, T. P.; Brown, H. R.; Hawker, C. *Macromolecules* **1996**, *29*, 6531.
(78) Lin, E. K.; Wu, W.-l.; Satija, S. K. *Macromolecules* **1997**, *30*, 7224.
(79) Zheng, X.; Rafailovich, M. H.; Sokolov, J.; Strzhemechny, Y.; Schwarz, S. A.; Sauer, B. B.; Rubinstein, M. *Phys. Rev. Lett.* **1997**, *79*, 241.
(80) Rossler, E. *Phys. Rev. Lett.* **1990**, *65*, 1595.
(81) Fujara, F.; Geil, B.; Sillescu, H.; Fleischer, G. *Z. Phys. B* **1992**, *88*, 195.
(82) Chang, I.; Fujara, F.; Heuberger, B. G. G.; Mangel, T.; Sillescu, H. *J. Non-Cryst. Solids* **1994**, *172*−*174*, 248.
(83) Hansen, C.; Stickel, F.; Berger, T.; Richert, R.; Fischer, E. W. *J. Chem. Phys.* **1997**, *107*, 1086.
(84) Hansen, C.; Stickel, F.; Richert, R.; Fischer, E. W. *J. Chem. Phys.* **1998**, *108*, 6408.
(85) Gotze, W.; Sjogren, L. *Rep. Prog. Phys.* **1992**, *55*, 241.
(86) Ngai, K. L.; Magill, J.; Plazek, D. *J. Chem. Phys.* **2000**, *112*, 1887.
(87) Plazek, D. J.; Magill, J. H. *J. Chem. Phys.* **1966**, *45*, 3038; **1968**, *49*, 3678.
(88) Stickel, F.; Fischer, E. W.; Richert, R. *J. Chem. Phys.* **1995**, *102*, 6251.
(89) DeMaggio, G. B. Ph.D. Thesis, The University of Michigan, 1997.
(90) Ngai, K. L.; Plazek, D. J. In *Physical Properties of Polymers Handbook*; Mark, J. E., Ed.; American Institute of Physics: Woodbury, NY, 1996; p 349.

MA035579A